Thermocouple response time estimation and temperature signal correction for an accurate heat flux calculation in inverse heat conduction problems

A.V.S. Oliveira, A. Avrit, Michel Gradeck

Version of Record: https://www.sciencedirect.com/science/article/pii/S0017931021014976
Manuscript_82bf6058bfe5e5122cf45dd07931d28a

Thermocouple response time estimation and temperature signal correction for an accurate heat flux calculation in inverse heat conduction problems

A. V. S. Oliveira[a], A. Avrit[a], M. Gradeck[a,*]

[a] *Université de Lorraine, CNRS, LEMTA, F-54000 Nancy, France*

Abstract

Many heat transfer processes do not allow temperature measurements with advanced instruments like IR cameras, and thus require the use of thermocouples – often inserted sheathed thermocouples – in order to measure the temperature in some key-regions. Nevertheless, thermocouples have an intrinsic response time that can dampen substantially temperature measurements and, when applicable, affect heat flux estimations by inverse methods. In this study, a thermocouple measurement correction method is proposed, especially for fast thermal transients like quenching, to avoid underestimation of the boundary heat fluxes due to delayed temperature responses. A simplified energy balance at the hot junction allowed modeling the temperature measurement by a thermocouple, in which heat losses and the response time were taken into account so they can be estimated using the least squares method on experimental data. A series of tests was performed to validate the present method with a heated jet impinging on a copper body instrumented with two thermocouples: one ungrounded and sheathed, then with high response time ("slow"); and another with exposed welded wires, hence with low response time ("fast"). After having estimated the slow thermocouple response time and heat loss parameters, the model allowed a good reconstruction of the fast thermocouple signal using the slow thermocouple measurements. Also, the heat flux estimation by the inverse method using the reconstructed signal resulted in practically the same results obtained using the fast thermocouple data. A parametric sensitivity analysis showed the heat loss parameters can be neglected for heat flux estimations, while simulations showed that temperature noises degrade the response time estimation but data filtering can mitigate this noise effect. Finally, the present method was applied to a large scale jet-cooling of a hot plate – near industrial conditions – and showed a substantially higher dissipated heat flux than the initially estimated. In fact, the results using reconstructed signals demonstrated that the heat flux dissipated by the jet has a higher dependence on the jet Reynolds number than the observed with the original thermocouple measurements, showing how important the temperature measurement correction is to evaluate fast thermal processes.

Keywords:

Inverse method, Instrumentation, Maximum heat flux, Contact resistance, Quenching, Jet impingement, Spray cooling

Nomenclature

*Corresponding author
Email address: michel.gradeck@univ-lorraine.fr (M. Gradeck)

Greek letters

β	model parameter
λ	thermal conductivity
Φ	heat flow rate
ρ	density
σ	noise level (standard deviation)
τ	thermocouple response time
θ	temperature difference
ε	temperature noise
φ_w	heat flux at the wall
ξ	thermal resistance ratio

Roman letters

$\mathbf{D}$	result vector
$\mathbf{S}$	sensitivity matrix
A	area
a	thermal diffusivity
b	polynomial coefficient
C	thermal capacity
c_p	specific heat
C.V.	control volume
d	diameter
E	relative error
e_{RMS}	RMS error
f	function
k	time step
$K_{1,2,3}$	least-squares solutions
L	length
m	mass
m_p	number of data in polynomial
n_G	number of Gaussian filter points
n_p	polynomial order
n_{fts}	number of future time steps
p	Laplace parameter
Q	water flow rate
R	thermal resistance
Re_j	jet Reynolds number
RRE	reduced radiation error
T	temperature
t	time
w	Gaussian filter weight
X	thermal impedance
x	position
Z	inverse Laplace solution

Subscripts

0	initial
amb	ambient
e	equivalent
fast	fast thermocouple
g	gas
max	maximum
min	minimum
P	point
Rec	reconstructed signal
ref	reference
slow	slow thermocouple
TC	thermocouple
un	undisturbed

1. Introduction

Thermocouples are one of the most used temperature sensors by engineers because, for most applications, it is sufficiently accurate, accessible and easy to use with modern data acquisition systems. However, it is common to see analyses based on thermocouple results as if they measured the actual temperature of the area of interest. More precisely, when inserting a thermocouple into a medium, there is an energy balance of the thermocouple's hot-junction with the entire system that results in a certain temperature, the one that we measure, that can differ from the medium temperature that we desire to measure.

This particular problem is very well known by the heat transfer community dealing with radiation and conduction, thus many correction methods have being created to mitigate it. Lemaire and Menanteau [1] compared different radiation correction methods in a combustion environment for high heating rates, analyzing not only the accuracy of each method but also their feasibility and sensitivity. Pope et al. [2] analyzed the error of thermocouple measurements when it is inserted perpendicularly to the isotherms in the body because of a thermal bridging effect in the sensor, which does not occur when the thermocouple is inserted parallel to the isotherms. They proposed a correction method for the perpendicular instrumentation based on a numerical model of the experiment. Terzis et al. [3] proposed a correction method for thermocouple measurements in a hot gas, based on the sensor response time which was obtained in a prior experiment where the gas temperature is known. Hashemian et al. [4] also proposed an *in situ* calibration experiment to determine the thermocouple response time that consists of applying a controlled electrical current through the thermocouple, heating it and then measuring its relaxation when put in a cooler fluid. Zhou et al. [5] tested different correction methods for the measurement of flame temperature using thermocouples with different bead diameters: among these methods is the extrapolation of a second-degree equation of the temperature reading with the thermocouple diameter proposed in 1968 by Daniels [6]. Brohez et al. [7] showed that radiation can affect the gas temperature measurement with thermocouples in steady-state conditions if the temperature difference between the gas and the surroundings is very different. They proposed a simple correction parameter, named reduced radiation error (RRE), that is used in the difference between two temperature measurements by thermocouples with different diameters. Most of these correction models are presented in Table 1.

In summary, we notice with these examples the existence of two main sources for the difference between the thermocouple measurement and the medium temperature: the first, in both transient and steady-state conditions, is due to conjugated heat transfer phenomena (convection, radiation and conduction) resulting in the hot-junction of the thermocouple being in thermal imbalance with the medium; the second, only in transient processes, is due to the thermocouple's response time for temperature change. A third source of error is the temperature field distortion due to the thermocouple holes in the sample [8], a typical instrumentation disturbance of the phenomena that adds a deterministic uncertainty to the measurement [9]; however, this source is not analyzed in the present study.

In studies involving fast temperature transients, such as cooling of hot metals with jets and sprays or transient boiling heat transfer, thermocouple measurements are usually used as the true temperature because, to the authors' knowledge, no correction has been proposed so far for these applications. Moreover, it is practically impossible to use physical models, multiple thermocouples or *in situ* calibration tests, i.e. the main correction methods used in the aforementioned examples. Physical models do not allow a precise estimate of the thermocouple response time because many constructive factors can influence the contact quality between the thermocouple and the sample, like

Table 1: Thermocouple response and correction models proposed by researchers cited in this study.

Authors	Correction model	Observations
Brohez et al. (2004) [7]	$RRE = \frac{T_g - T_{TC,1}}{T_{TC,2} - T_{TC,1}}$	The two thermocouples (1 and 2) have different diameters. RRE is found merging the energy balance equations for each thermocouple.
Daniels (1968) [6]	$T_{TC} = K_1 + K_2 d_{TC} + K_3 d_{TC}^2$	Using thermocouples with different diameters, one could find the least-squares solutions (K_1, K_2 and K_3) and, then, the gas temperature $T_g = K_1$ when $d_{TC} = 0$.
Pope et al. (2021) [2]	$E(t) = \frac{T_{un}(t) - T_{TC}(t)}{T_{un}(t) - T_{amb}}$	$E(t)$ is found by numerical simulations with and without the thermocouple.
Terzis et al. (2012) [3]	$T_g(t) = T_{TC}(t) + \tau \frac{dT_{TC}}{dt}$	τ is obtained experimentally by imposing a gas flow and finding time for 63.2% change in the temperature measurement.
Woodfield and Monde (2009) [10]	$T_{TC}^k = T_P^k + (T_{TC}^k - T_P^k) \exp\left(-\frac{\Delta t}{\tau}\right)$	They proposed imposing a τ in the calculations to simulate the thermocouple measurement and estimate the inverse method time resolution.

geometry, contact pressure, presence of microswarf after machining (if the thermocouple is inserted into a hole) or quality of the welding (if this method is adopted). Using thermocouples with different sizes is not a solution because quenching experiments usually involve significant temperature gradients, so the thermocouples would not measure the same temperature, and we would increase the thermal field disturbance by instrumentation. Finally, *in situ* characterization is normally not feasible because either the target temperature is unknown or, if using the method proposed by Hashemian et al. [4], the medium temperature near the thermocouple could change and affect the response time estimation. Although no correction method is currently available, Woodfield and Monde [10] proposed to evaluate the uncertainty of inverse heat conduction solutions to estimate the heat flux at the boundary that includes the thermocouple response time, among other parameters; however, this uncertainty is evaluated as spatial and time resolutions of the results, not an uncertainty of the estimated heat flux value.

Although several recent studies involving fast transient heating and cooling use infrared thermography as temperature measurement technique [11–13], thermocouples are still the preferred temperature sensor in most investigations. As Oliveira et al. [14] presented in their jet cooling experiment study, the lack of a correction method prevents a comparison between the many experimental results available in the literature. For example, different hot-metal jet cooling tests in similar conditions provided very different maximum heat fluxes at the impact location. Nobari et al. [15] found 11.3 MW/m^2 using exposed thermocouple wires with 0.25 mm diameter that were directly spot-soldered to the sample, a maximum heat flux value slightly lower than the one found by Gradeck et al. [16] (12.5 MW/m^2) using back-surface infrared thermography. Karwa and Stephan [17] found about a 9 MW/m^2 peak heat flux using

a grounded sheathed thermocouple with 0.5 mm diamter inserted into a hole in the sample with a thermal paste to improve the thermal contact. In turn, Oliveira et al. [14] and Wang et al. [18] found a maximum heat flux of approximately 4.8 MW/m^2, the former using a ungrounded sheathed thermocouple with 1 mm diameter that was inserted into a hole without thermal paste, and the latter using a sheathed thermocouple (no mention if grounded or not) with 3 mm diameter also inserted into a hole but with thermal paste. The most probable reason for those very different results is the thermocouple response time effect. This effect is highlighted in Fig. 1 where we present simulated thermocouple measurements for different response times τ (using Eq. 3 to be presented in the next section) of the 1D heat conduction problem presented in Appendix A. The imposed heat flux at the boundary φ_w is shown in Fig. 1a, which was used by Nobari et al.[15] in one of their experiments. The simulated temperature measurements are dampened as the response time increases (Fig. 1b), decreasing substantially the cooling rate. In fact, the difference between the real temperature (for $\tau = 0$) and those measured if $\tau \neq 0$ reached values higher than 100 °C even for small response times Fig. 1c. The response time effect is noticeable when using an inverse method (see Appendix A) to estimate the heat flux at the boundary from the temperature measurements; we use the notation $\hat{\cdot}$ for estimated variables, thus here $\hat{\phi}_w$ is the estimated heat flux at the wall. The estimated maximum heat flux drops to half of the imposed boundary value if $\tau = 0.25$ s, which is slightly higher than the typical response time of a 1 mm sheathed thermocouple.

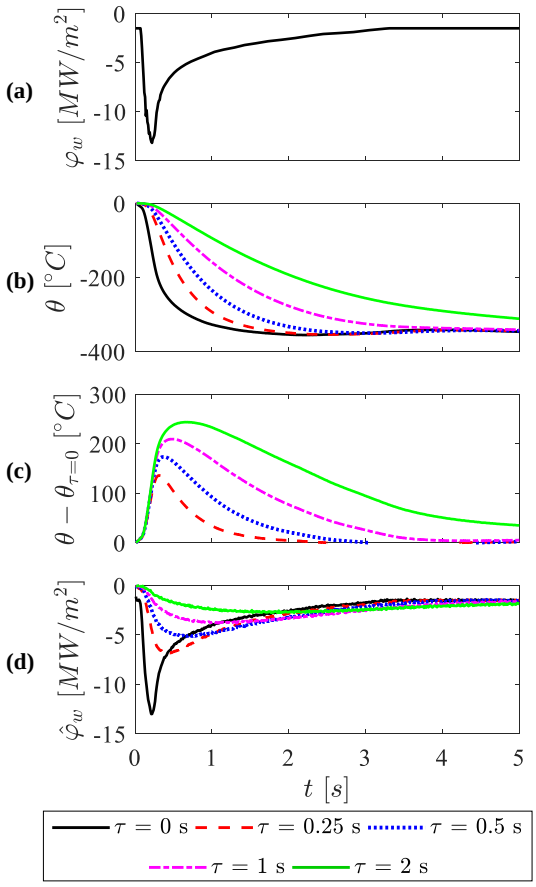

Figure 1: Presentation of the thermocouple response time problem with a 1D heat conduction simulation using Eq. 3: a) imposed heat flux as boundary condition; b) temperature evolution over time for each response time; c) difference between temperature evolutions with and without response time; d) estimated heat flux using each thermocouple measurement in (b).

A correction method for the thermocouple measurements in fast transient experiments becomes necessary to have accurate estimates of the heat flux when solving inverse heat conduction problems. We present in this study a procedure to obtain experimentally the thermocouple response time in a prior small-scale calibration test reproducing the instrumentation method to be used in the main experimental campaign. More precisely, the temperature response from a slow thermocouple used in the main experiments is compared with the one obtained with a fast thermocouple in this calibration test, so a relative response time is obtained and the slow thermocouple measurements can be corrected to provide results as if the sample were instrumented with the fast thermocouple. First, we present a model for the thermocouple response, considering both the response time and heat loss parameters at the hot junction, and the corresponding least squares method to estimate these coefficients. We apply the proposed method to experimental results of single-phase jet impingement heat transfer for different configurations. Then we analyze the importance of the heat loss parameters and investigate different parametric effects like thermocouple noise and data filtering. Finally, we use the present correction method in experimental data of hot-metal jet cooling by Oliveira et al. [14] to demonstrate how this prior calibration experiment can improve the heat flux estimation in large scale experiments. The MatLab code with two examples of temperature measurements is available in the supplementary material and Appendix B explains how to use the code.

2. Thermocouple response modeling

2.1. Thermocouple response time (τ)

In ideal conditions, the temperature T_{TC} measured by a thermocouple should be the same as the temperature T_P that we desire to measure at a given point P in the body. Nevertheless, this does not happen in real applications because there is always an equivalent thermal resistance R_e between P and the thermocouple hot junction, assumed constant in this study, as well as the thermocouple thermal inertia given by its equivalent capacity $C_e = m_e c_{p,e}$ that is proportional to a equivalent mass m_e and a equivalent specific heat $c_{p,e}$ of the hot junction. The word "equivalent" is used to describe these parameters because the method adopted to place or attach the thermocouple to the body can affect them, as well as the thermocouple characteristics. For example, a system using an ungrounded sheathed thermocouple inserted in the body will have different thermal resistances than another where the thermocouple wires are welded or soldered to the body. Another example would be tin-soldering the thermocouple to the body, which adds mass to the system and affects its thermal capacity.

If we neglect at first the heat conduction within the thermocouple (the control volume in Fig. 2 with $R_{TC} \to \infty$), its temperature response T_{TC} can be very simply modeled with an electrical analogy - considering a heat flow rate Φ from P to the thermocouple hot junction - as follows:

$$\Phi = \frac{T_P - T_{TC}}{R_e} = C_e \frac{dT_{TC}}{dt} \tag{1}$$

If T_P is constant, which is the case, for example, in water bath immersion tests to measure the thermocouple response time (method commonly used by thermocouple suppliers), the solution for the thermocouple measurement evolution is as follows:

$$T_{TC} = T_P + (T_{TC,0} - T_P) \exp\left(-\frac{t}{\tau}\right) \tag{2}$$

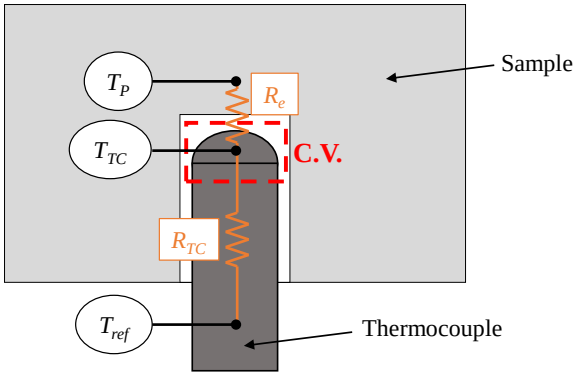

Figure 2: Schematic drawing of energy balance at the thermocouple hot junction, which is the control volume of the problem.

where $T_{TC,0}$ is the thermocouple measurement at $t = 0$ and $\tau = R_e C_e$ is a characteristic time known as the thermocouple response time. Some intuitive parametric effects become easier to understand when looking at the response time as a product of the equivalent thermal resistance and heat capacity:

- Larger thermocouples have higher mass, so the response time is higher;
- Spot-welding the thermocouple wires to the body has lower mass and thermal resistance than inserting a sheathed thermocouple into the body, so the response time is lower for the first case;
- Incomplete insertion of a sheathed thermocouple into the body adds a thermal resistance related to the confined air, increasing the response time;
- For inserted sheathed thermocouples, the surface finish, morphology match and contact pressure in the body-thermocouple contact affect the thermocouple response time.

In applications where T_P is also transient, as during jet or spray cooling experiments, the thermocouple response can be modeled iteratively either solving Eq. 1 using an hypothesis of T_P being constant by parts (which results in Eq. 2 with $t = \delta t$, where δt is the sampling time – see Woodfield and Monde [10] model in Table 1) or varying linearly during the sampling time [10]. Another option is the use Eq. 1 as it is presented (but with the response time τ) for each time step k and use any efficient, stable method to estimate the temperature derivative dT_{TC}/dt, similarly to Terzis et al. [3] model, hence:

$$T_{TC}^k = T_P^k - \tau \left. \frac{dT_{TC}}{dt} \right|_{t_k} \tag{3}$$

2.2. Energy balance with heat loss

In the case of the thermocouple being inserted perpendicular to isotherms, there is heat conduction from the hot junction to the thermocouple body (sheath or wire) if $T_{TC} > T_{ref}$ (Fig. 2) that can also affect the temperature measurements [2]. In this case, the energy balance in the control volume at the hot junction becomes:

$$\frac{T_P - T_{TC}}{R_e} - \frac{T_{TC} - T_{ref}}{R_{TC}} = C_e \frac{dT_{TC}}{dt} \tag{4}$$

where R_{TC} is the thermal resistance between the thermocouple hot-junction position and a reference temperature T_{ref}. Both R_{TC} and T_{ref} are considered constants in this model. This equation can be applied to transient applications after multiplying the entire equation by R_e, which leads to:

$$T_P^k - T_{TC}^k = \tau \frac{dT_{TC}}{dt}\Big|_{t_k} + \xi \left(T_{TC}^k - T_{ref}\right) \tag{5}$$

$\xi = R_e/R_{TC}$ being a thermal resistance ratio.

If $\xi \simeq 0$, i.e. $R_e \ll R_{TC}$, Eq. 5 becomes Eq. 3. Nevertheless, ξ can be significant as its order is actually between 10^{-4} and 1 according to the orders of magnitude of each resistance. For the contact resistance, $R_e.A \sim 10^{-6} - 10^{-3}$ K m^2 W^{-1} [19, 20], where A is a characteristic area. Meanwhile, we have for the thermocouple conductive resistance $R_{TC}.A = L_{TC}/\lambda_{TC} \sim 10^{-3} - 10^{-2}$ K m^2 W^{-1}, A still being a characteristic area and considering the effective length $L_{TC} \sim 10^{-2} - 10^{-1}$ m and the thermal conductivity $\lambda_{TC} \sim 10$ W m^{-1} K^{-1}. In regards to the reference temperature T_{ref}, this could be the ambient temperature T_{amb}, the sample initial temperature T_0 if it is not the same as T_{amb}, or even any value in between. One could already note that both ξ and T_{ref} are not constants in an experiment, but this assumption is necessary at first for correcting the thermocouple measurement ; it is also necesary in order to demonstrate that the last term in Eq. 5 can be neglected in the signal reconstruction for estimating the heat flux as boundary condition in inverse heat conduction problems (see section 3.3).

2.3. Estimating the temperature derivative

If data were smooth and noiseless, as in a numerical simulation, a simple finite difference method would be sufficient to calculate the temperature derivative. However, experimental temperature measurements always have an embedded noise that is greatly amplified when calculating the derivative by finite differences [21]. For this reason, a regularization method becomes necessary to reduce the noise effect of the derivative calculation, several approaches being studied and compared by Breugel et al. [21] and Knowles and Renka [22]. In this study, we chose to use a relatively simple approach based on the classical method by Savitzky and Golay [23], who proposed filtering noisy data by estimating the true value at k using a polynomial fit for a moving window containing $2m_p+1$ data. Therefore, we have the following polynomial $f(t)$ of order n_p:

$$f_{n_p}(t) = \sum_{j=0}^{n_p} b_j t^j \tag{6}$$

whose coefficients b_j can be found by least squares using the $2m_p + 1$ points in the window that is centered at t_k. Our approach consists of filtering the temperature derivative at a time step k, which can be found by calculating t_k using the derivative of the polynomial at the center of the window $(m_p + 1)$, i.e.:

$$f'_{n_p}(t_k) = \sum_{j=1}^{n_p} j b_j t_{m_p+1}^{j-1} \tag{7}$$

Choosing a very little order for the polynomial could result in a poor fitting curve in fast transients, while setting a very high order, but still limited to $n_p \leq 2m_p$, could provide an overfitted function that fluctuates with the noise. To achieve a more stable solution, we estimated the temperature derivative at the time step k for Eqs. 3 or 5 using

several fitted polynomial orders (usually n_p from 3 to 6 for $m_p = 15$) and calculating their mean derivative, which means:

$$\frac{dT_{TC}}{dt}\Big|_{t_k} = \frac{1}{4}\sum_{n_p=3}^{6} f'_{n_p}(t_k) \tag{8}$$

There is a substantial noise amplification of the temperature derivative when the thermocouple response time is long. For this reason, this derivative calculation is performed using the thermocouple measurement filtered as well with a Gaussian filter. As we present in the results, this prior filtering did not affect the thermocouple response time estimation nor the thermocouple signal reconstruction.

2.4. Estimating τ, ξ and T_{ref} with experimental data

Differently from a bath immersion test, where the target temperature T_P is known (bath temperature), the real temperature that the thermocouple is supposed to measure in a transient application is undetermined. Therefore, depending on the application, it can be impossible to estimate the thermocouple true response time experimentally. We can overcome this problem by finding a response time of the thermocouple (named "slow" in this study) used in a main large-scale experiment compared to a much faster thermocouple (named herein "fast") whose response time is assumed zero. This hypothesis in evidently not true because, as already mentioned, any thermocouple has a response time. Nevertheless, depending on the application and if, for example, its wires are very thin and it is well welded to the sample, its response time can be negligible.

Not only the thermocouple response time τ must be estimated but also the heat loss terms ξ and T_{ref} for a complete characterization of the instrumentation. Identifying the slow and the fast thermocouple measurements respectively as T_{TC} and T_P and using a temperature difference $\theta = T - T_0$ where T_0 is the initial temperature of the sample, we can rearrange Eq. 5 as follows:

$$\theta^k_{fast} - \theta^k_{slow} = \tau\frac{d\theta_{slow}}{dt}\Big|_{t_k} + \xi\theta^k_{slow} - \xi\theta_{ref} \tag{9}$$

and find the matrix equation below with the N_t temperature measurements:

$$\mathbf{S}\begin{bmatrix}\hat{\tau}\\ \hat{\xi}\\ \hat{\xi}\hat{\theta}_{ref}\end{bmatrix} = \mathbf{D} \tag{10}$$

where:

$$\mathbf{S} = \begin{bmatrix} \frac{d\theta_{slow}}{dt}\Big|_{t=\delta t} & (\theta_{slow})_{t=\delta t} & -1 \\ \frac{d\theta_{slow}}{dt}\Big|_{t=2\delta t} & (\theta_{slow})_{t=2\delta t} & -1 \\ \vdots & \vdots & \vdots \\ \frac{d\theta_{slow}}{dt}\Big|_{t=N_t\delta t} & (\theta_{slow})_{t=N_t\delta t} & -1 \end{bmatrix} \tag{11}$$

$$\mathbf{D} = \begin{bmatrix} (\theta_{fast} - \theta_{slow})_{t=\delta t} \\ (\theta_{fast} - \theta_{slow})_{t=2\delta t} \\ \vdots \\ (\theta_{fast} - \theta_{slow})_{t=N_t\delta t} \end{bmatrix} \tag{12}$$

Thus, we estimate the response time of the slow thermocouple using the least squares method:

$$\begin{bmatrix} \hat{\tau} \\ \hat{\xi} \\ \hat{\xi}\hat{\theta}_{ref} \end{bmatrix} = \left(\mathbf{S}^T\mathbf{S}\right)^{-1}\mathbf{S}^T\mathbf{D} \tag{13}$$

where $\hat{\tau}$ is the estimated response time, $\hat{\xi}$ is the estimated thermal resistance ratio and $\hat{\theta}_{ref}$ is the estimated reference temperature difference. Therefore, we need a calibration step to estimate these parameters knowing *a priori* both thermocouple responses. We validate the estimated parameters values in a supplementary experiment, with a different thermal input sequence, where we estimate the fast thermocouple response with the following expression:

$$\hat{\theta}_P^k = \theta_{TC}^k + \hat{\tau}\frac{d\theta_{TC}}{dt}\bigg|_{t_k} + \hat{\xi}\left(\theta_{TC}^k - \hat{\theta}_{ref}\right) \tag{14}$$

These calibration and validation steps for the parameters estimation is better explained in the next section with an experimental application of the present method.

The advantage of using physical models with estimated parameters is that hidden characteristics of the system that are difficult to model, like surface roughness and construction or assembly imperfections (as some examples listed in section 2.1), are comprised in the estimated parameters, especially in the thermocouple response time. Nevertheless, we assumed all the thermal resistances are constant, which means, for example, that assembly characteristics are unchanged during the thermal transient and the thermophysical properties are also constant. Even though these assumptions may not be true in some cases, the estimated parameters are still the closest to the true "mean" value and, consequently, the best fit of the model with the experimental data. In the present study, we fixed constant thermal resistances because it provides a very simple model that not only is easy to work with but also presented satisfactory results, as shown in the next sections. Nevertheless, the effect of temperature-dependent processes (like change in the thermocouple-wall contact resistance due to the material thermal expansion or contraction) and thermophysical properties should be evaluated in future investigations, possibly using numerical simulations, to obtain quantitative results of the model accuracy in these conditions.

3. Application with a jet impingement experiment

Figure 3 illustrates how the present method can be applied in fast-transient heat transfer experiments. Let us consider a main experimental campaign with large-scale experiments, possibly in near-industrial or application conditions. These tests usually involve large test samples that are difficult to machine and instrument. Moreover, the test conditions and environment are usually rough, involving high temperature gradients and thermal stresses that make virtually impossible the use of sensible and delicate instrumentation like thin spot-welded thermocouples. For this reason, it is usually preferred to use sheathed thermocouples with relatively large diameters (1 mm or larger) that can withstand the test conditions and be used several times. Nevertheless, it means the temperature measurements will be delayed, (1) in Fig. 3, and affect the heat flux estimations by inverse methods, as discussed in the introduction.

To estimate the thermocouple response time with Eq. 13, we need to have measurements from a fast thermocouple for the same point of the original (and slow) thermocouple. Therefore, one can reproduce the large-scale experimental instrumentation method in a small sample, including the use of the original slow thermocouple, but adding a fast

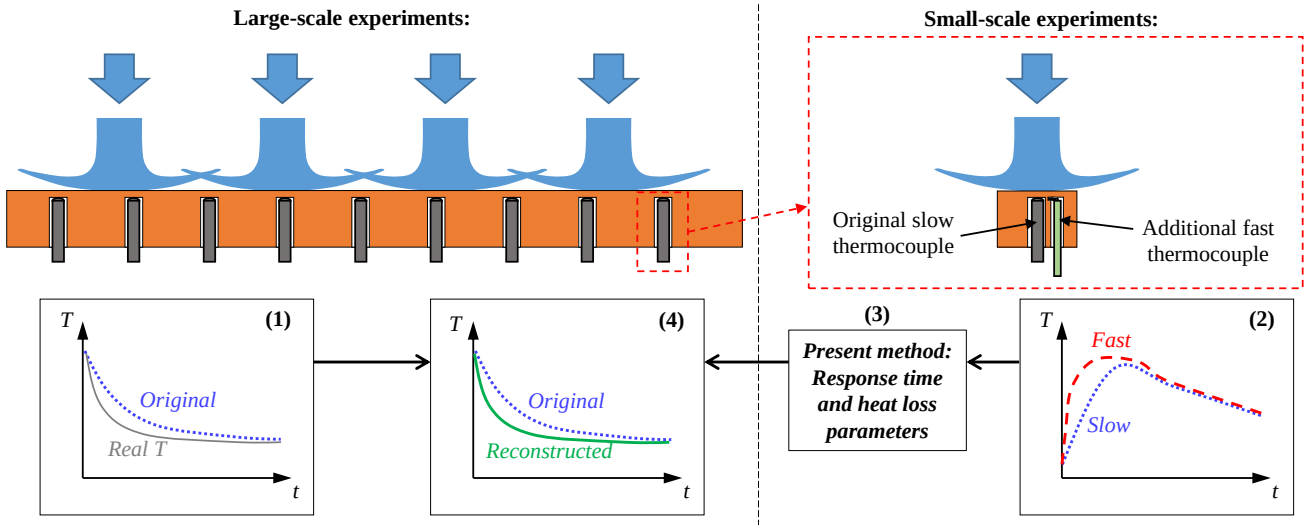

Figure 3: Using the present method in a small-scale experiment to correct temperature measurements in a large-scale experiment: 1) original delayed temperature measurements by slow thermocouples; 2) small-scale test reproducing the large-scale instrumentation; 3) estimate of the slow thermocouple response time; and 4) reconstruction of the thermocouple signal in the large-scale experiment using the estimated response time.

thermocouple and putting both hot-junction points close to each other to measure, at principle, the same temperature. In this experiment, we can use, for instance, a single hot jet impinging the test section and measure both responses, certainly observing a faster response with the fast thermocouple ((2) in Fig. 3), or any other method where the temperature gradients are not very high to avoid damaging the thermocouple and to sustain the hypothesis that both thermocouples measure practically the same temperature. Then, these measurements would be used in Eq. 13 to estimate the model parameters, (3) in Fig. 3, which, in turn, would be applied in Eq. 14 to reconstruct the temperature measurements in the large-scale experiment ((4) in Fig. 3). As we demonstrate later in this paper, this signal reconstruction improves substantially the accuracy of the heat flux estimate with an inverse method.

Although we used jets in the illustration of Fig. 3, the large-scale experiment could involve any efficient heat transfer process, like jet impingement, spray cooling, nucleate boiling, condensation, or others. In turn, the small-scale experiment does not have to use the same heat transfer process to find the model parameters – it could be, for example, a hot air impacting the test section – because the model is indifferent to the phenomena taking place at the boundary.

3.1. Experimental apparatus and procedure

Figure 4a presents an illustration of the experimental apparatus and the test section used in the experiments to validate our method of estimating the thermocouple response time and heat loss parameters, which consists of a water jet-impingement heating a copper piece. This is the same apparatus used by Lecoanet et al. [24], who presents it in detail, so here we introduce the main equipment only. The water jet was supplied at 70°C ± 1°C by a hydraulic circuit composed of a tank with pre-heated water, a volumetric pump, a flowmeter and an injection nozzle with 6 mm diameter. The water flow rate was fixed at 12 l/min for all the tests. To ensure the water temperature leaves the nozzle at the desired temperature, the fluid flows for one hour through a bypass close to the nozzle at the desired flow rate. The experiment starts by redirecting the flow to the test section using an electronic three-way valve. A data

acquisition system receives all the measurements signals; more precisely, for the water temperature, rotation speed of the volumetric pump, water flow rate and temperature measurements in the test section. The copper part is the target body that was instrumented with two type-K thermocouples: one named "slow" that is sheathed, ungrounded and inserted in the body from the bottom; and one named "fast" that had its two exposed wires (0.2 mm diameter) tin-soldered close to the tip of the slow thermocouple. The copper target is 28 mm long and its diameter in the long region is 6 mm, while in the upper part there is a 1-mm long slab with 16 mm diameter, which was necessary to ensure the sealing by compressing an FKM o-ring with the polycarbonate housing.

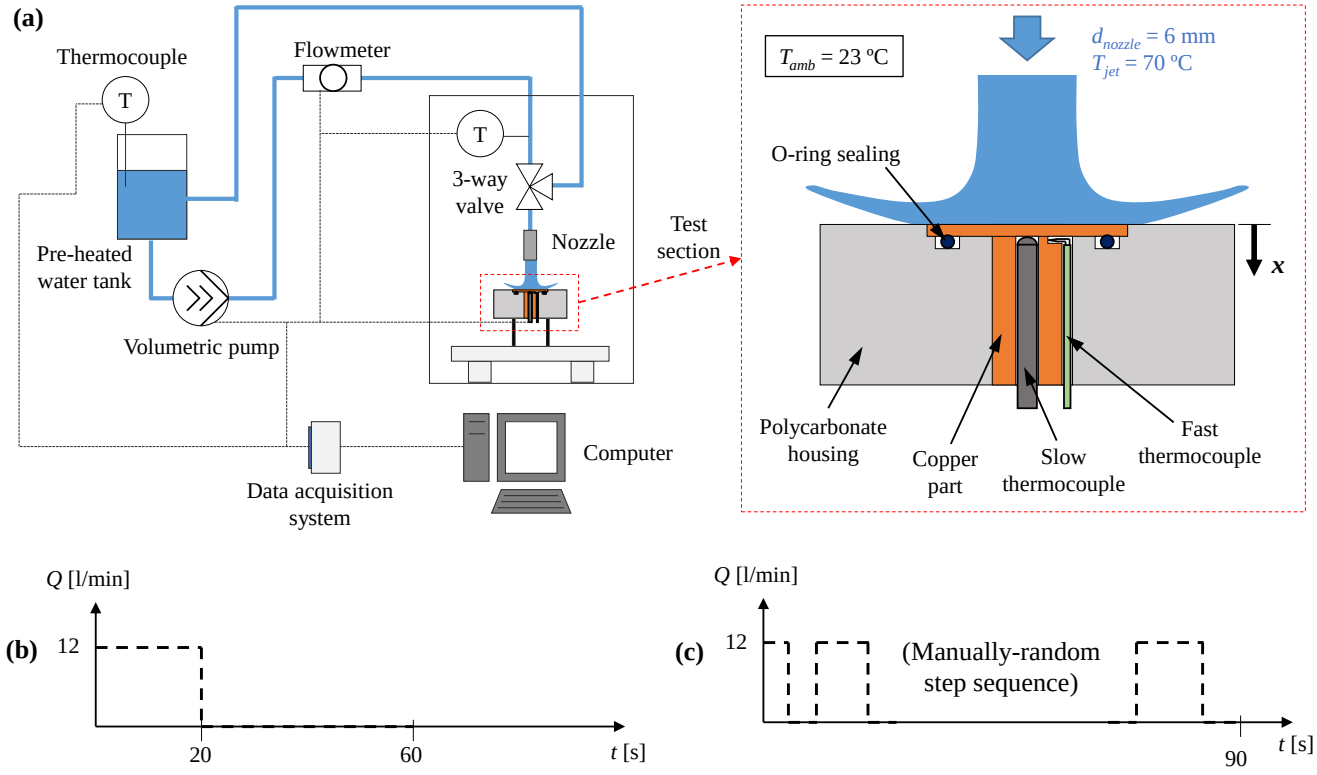

Figure 4: Illustration of the experiment and procedure: a) schematic drawing of the apparatus and the test section impinged by the jet; b) water flow rate profile for the calibration step; c) water flow rate profile for the validation step.

We used two different diameters for the slow thermocouple, 1 and 3 mm, and two different thermocouple insertion conditions with the 1-mm thermocouple, complete and incomplete insertion, the latter meaning the thermocouple was displaced by 1 mm from the hole tip (Table 2). These three test conditions allow to evaluate different response times. The increase in the thermocouple diameter leads to a growth of the response time because of its higher mass, hence higher thermal inertia, while not inserting well the thermocouple increases the thermal contact resistance, which increases as well the response time. The hole diameter of the copper piece where the slow thermocouple was inserted is 0.1 mm larger than the thermocouple diameter, which means one sample was used for tests 1 and 2 and another one for test 3. We already present in Table 2 the number of calibration tests performed for each condition and the estimated response time $\hat{\tau}$ and heat loss parameters $\hat{\xi}$ and $\hat{\theta}_{ref}$, although we discuss these results later in this paper.

The experimental procedure consisted basically in injecting the water jet onto the copper sample, whose temperature started from ambient (about 25°C), and measure the temperature evolution of both thermocouples. For the

Table 2: Test conditions and estimated thermocouple response times.

Test	**Insertion condition**	d_{TC} [mm]	**Number of calibration tests**	$\hat{\tau}$ [s]	$\hat{\xi}$ [-]	$\hat{\theta}_{ref}$ [°C]
1	Complete insertion	1	5	0.35 ± 0.04	0.04 ± 0.01	17 ± 5
2	Incomplete insertion (1 mm displacement)	1	3	0.43 ± 0.02	0.06 ± 0.01	21 ± 1
3	Complete insertion	3	3	2.4 ± 0.3	0.05 ± 0.01	23 ± 2

calibration step, necessary for estimating the response time and heat loss parameters of the slow thermocouple with Eq. 13, the water injection was maintained for 20 s, resulting in the test sample heating, and stopped afterwards for the temperature decrease due to heat loss to the environment that lasted 40 s, which means a total of 60 s for this experiment (Fig. 4b). In turn, for the validation step, when the fast thermocouple signal is reconstructed using the estimated parameters with Eq. 14, the water flow was started and stopped manually and randomly for 90 s, which resulted in a sequence of heating-cooling processes with different durations (Fig. 4c).

3.2. Experimental results

We performed the calibration step several times for each test to have a fairly accurate estimated response time and verify the repeatability of the procedure. The estimated values are presented in Table 2 and the results behave as expected: $\hat{\tau}$ is shorter for test 1 where we used a well-inserted small-diameter thermocouple, slightly larger for test 2 where we used the same thermocouple but not completely inserted, and the largest with the large-diameter thermocouple. The uncertainty of $\hat{\tau}$ was between 6% and 12%.

Figure 5a presents examples of calibration test results, one for test 1 and another for test 3, with the temperature evolution of the fast and slow thermocouples, and a zoom in the first seconds for each test to highlight the delay of the slow thermocouple signal compared to the fast one. The difference between these two thermocouples is plotted in Fig. 5b: the largest difference occurs in the beginning of the sample heating when the temperature transient is the highest. This is also verified in Fig. 5c where we present the temperature derivative evolution for each thermocouple. Note that the temperature difference profile and the temperature derivative of the slow thermocouple are the only necessary information to estimate the response time with Eq. 13 if ξ was null. For test 1, since $\hat{\tau} = 0.33$ s, the delay of the slow thermocouple response is not so evident. Although the difference between the fast and slow thermocouple signals reach 8 °C at about 1 s, after 6 s this difference becomes much smaller. Similarly, the temperature derivative of both signals are significant until $t = 2$ s. This means that the useful values for the response time estimation is concentrated in the first seconds of the calibration test, hence the relaxation period has virtually no effect at this step. The same is observed with test 3 results, where there is a much larger difference between the fast and slow thermocouple measurements because the estimated response time is much higher in this condition ($\hat{\tau} = 2.4$ s). Although the validation of the estimated $\hat{\tau}$ must not be performed with the same experiment used in the calibration, we present in the plots of Fig. 5 results for the reconstructed signal ("Rec" in the legends) using Eq. 14. We discuss again the results of the signal reconstruction in the validation step but we can already remark that the reconstructed

signal matches well the transient of the fast thermocouple in the first seconds. This is more evident when looking at the difference between these signals in Fig. 5b and the derivative calculation in Fig. 5c for test 1. For test 3, where the response time is high, the reconstructed signal is much noisier, especially in the derivative calculation, which is a consequence of the derivative noise amplification during reconstruction (Eq. 14).

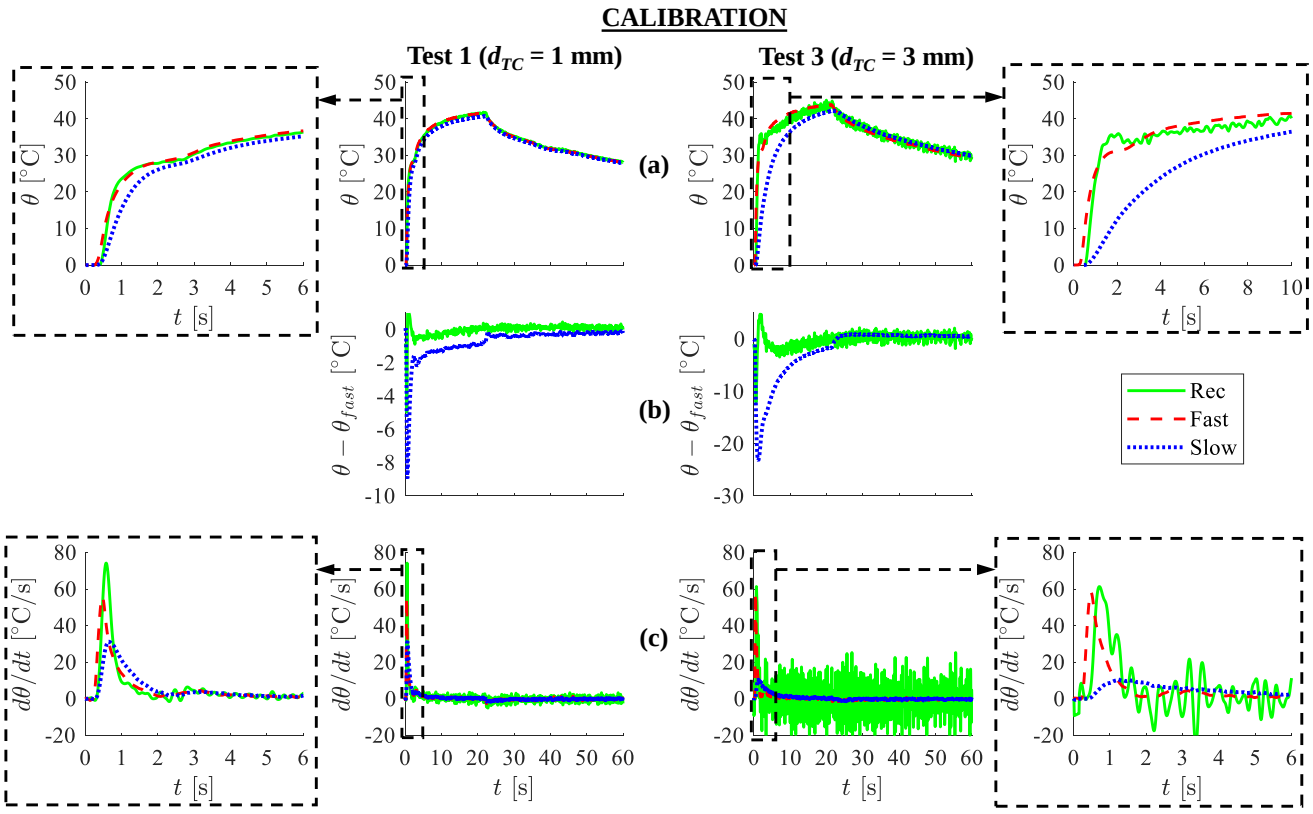

Figure 5: Experimental results (tests 1 and 3) for the calibration step to find the thermocouple response time and heat loss parameters: a) temperature evolution for each thermocouple and the reconstructed signal ("Rec"), with a zoom in the first seconds; b) temperature difference evolution between the fast thermocouple and the slow or reconstructed measurements; c) temperature derivative evolution for each thermocouple and the reconstructed signal, with a zoom in the first seconds.

Figure 6 presents the validation results where we use the estimated parameters to reconstruct the fast thermocouple signal (those presented in Table 2). The graphs are the same as that of Fig. 5, but the thermal input (the water flow rate) is a random sequence of steps instead of a single step (Fig. 4). For both presented tests, the reconstructed signal is much closer to the fast thermocouple signal than the original signal is, which can clearly be seen in Fig. 6b. Furthermore, the reconstructed signal was able to capture all the fast transitions that the fast thermocouple measured, which is easier to see in Fig. 6c with test 1 results where the reconstructed signal derivative is less noisy. For test 3, the only part where the reconstructed signal derivative is visibly non-zero is in the first transient where the peak is the highest. For the others, the noise is too high to visualize any significant variation in the derivative in the other transients, even though the reconstructed signal captured the heating processes as shown in Fig. 6a.

For inverse heat conduction problems, more important than reconstructing the thermocouple signal is estimating correctly the thermal input at the boundary, like the heat flux at the jet-impinged surface in our test case. We used a pseudo-analytical solution for 1D heat conduction (x-direction) in our experiment and Beck's regularization method

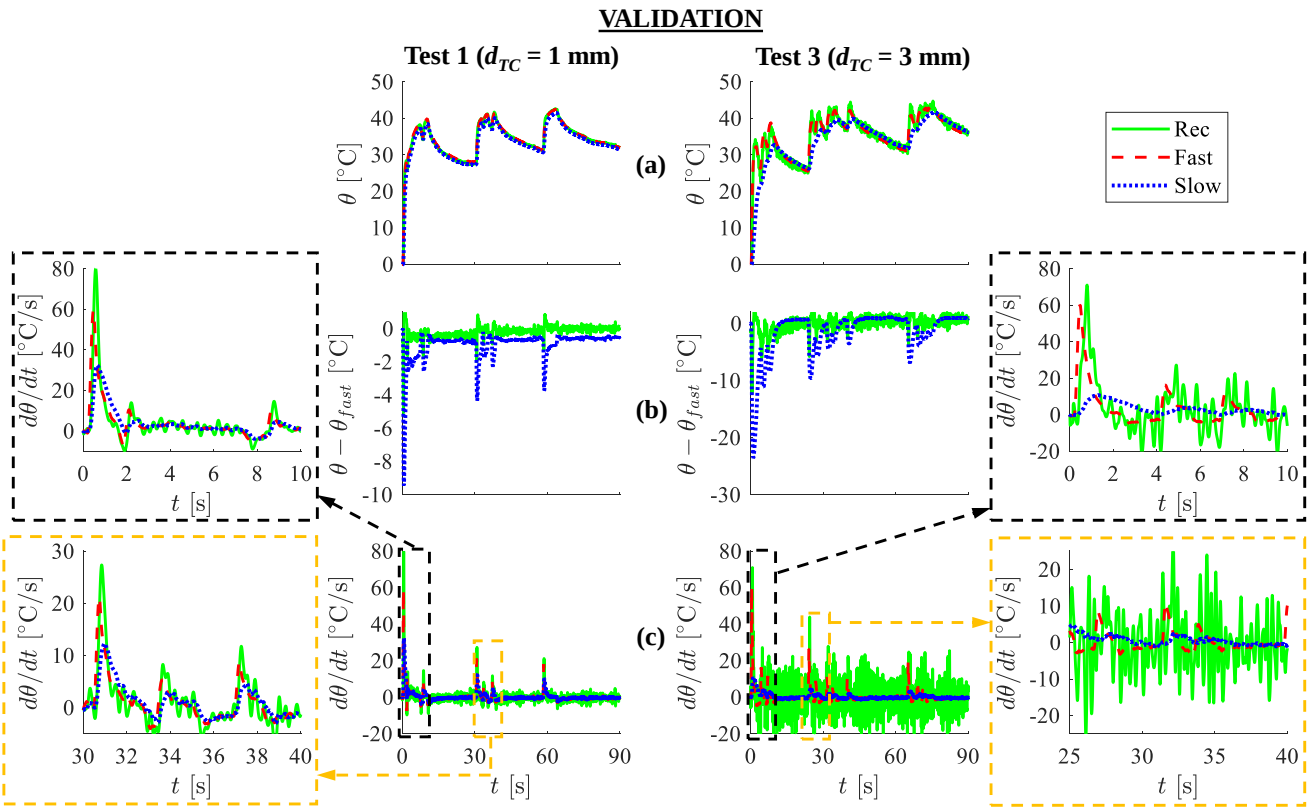

Figure 6: Experimental results (tests 1 and 3) for the validation step after having estimated the thermocouple response time and heat loss parameters: a) temperature evolution for each thermocouple and the reconstructed signal ("Rec"); b) temperature difference evolution between the fast thermocouple and the slow or reconstructed measurements; c) temperature derivative evolution for each thermocouple and the reconstructed signal, with zooms in different moments where the derivatives are higher.

to estimate this heat flux with the validation tests, which is presented in detail in Appendix A. We used different number of future time steps n_{fts} for each case, according to their noise level: for the original thermocouple signals (i.e. fast and slow), we set $n_{fts} = 5$, while for the reconstructed signal we used $n_{fts} = 15$ for tests 1 and 2 and $n_{fts} = 25$ for test 3 to compensate its high noise levels that was mentioned previously.

Figure 7 presents the evolution in the estimated heat flux $\hat{\varphi}_w$ for each thermocouple signal (fast, slow and reconstructed) and for each test case (1, 2 and 3), with zooms in the first seconds to better visualize each estimated curve at the highest peak. For tests 1 and 2 (Figs. 7a and b), where the response time is not very large, the values of the estimated heat fluxes using the fast and the slow thermocouples are close. In fact, the only substantial differences were found during the heating transients where the heat flux has a peak. For example, the calculated $\hat{\varphi}_w$ at the first peak using the slow thermocouple data is underestimated by 23.1% and 26.3% compared to the estimate using the fast thermocouple signal for test 1 and 2, respectively. Meanwhile, the estimated heat fluxes using the reconstructed signal is very close to the ones found using the fast thermocouple data, the difference between their first peaks being only 0.5% and 6.4% for tests 1 and 2, respectively. For the sake of experimental results validation, the peak heat fluxes we found in all the experiments, which is about 1.3 MW/m^2, are quite close to the value estimated by the correlation proposed by Womac et al. [25] for single-phase jet-impingement heat transfer at the impact location, which is approximately 1.6 MW/m^2.

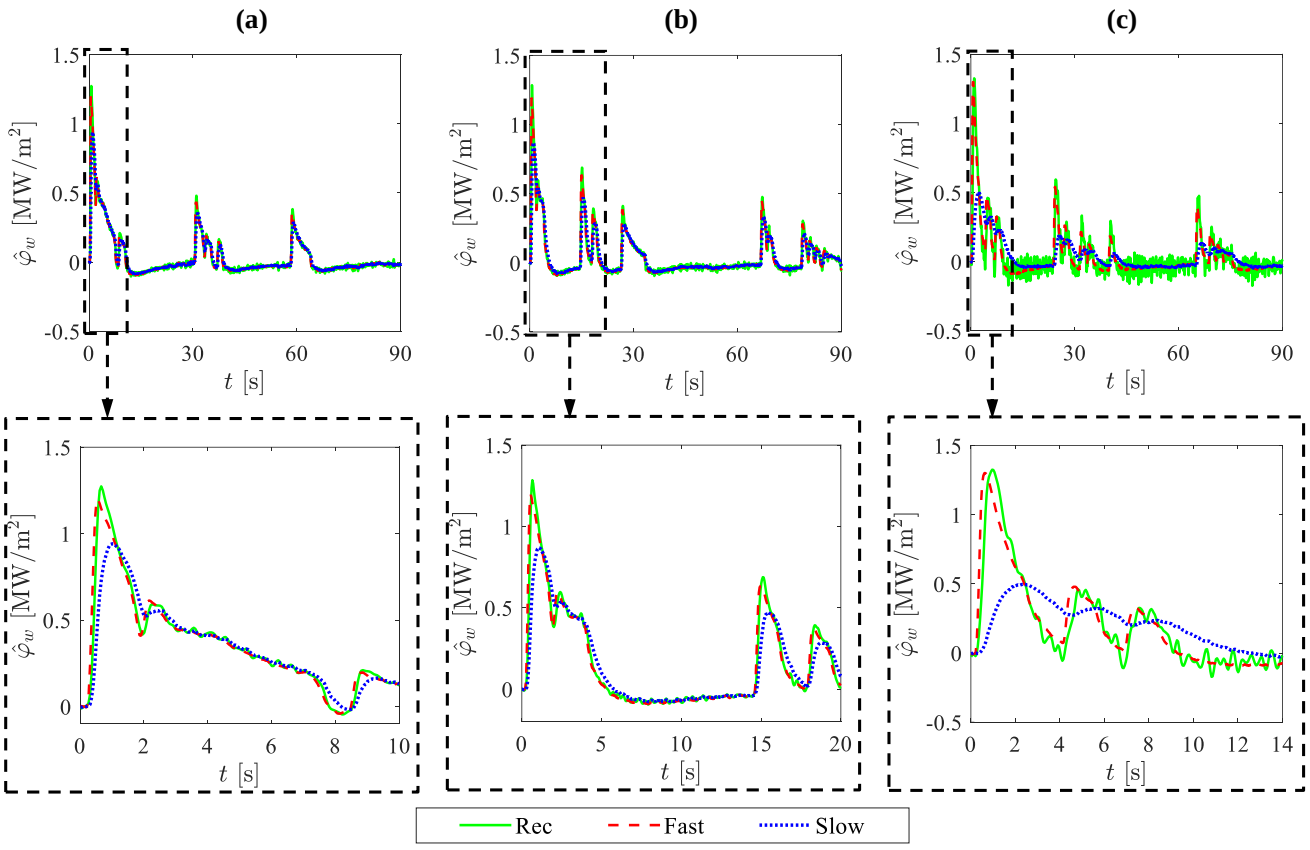

Figure 7: Results of the estimated heat flux over time at the jet-impinged surfaced: a) test 1; b) test 2; c) test 3.

The improvement in the heat flux estimate after reconstructing the thermocouple signal is even clearer for test 3 (Fig. 7c). The high response time of the slow thermocouple filters considerably the temperature transients and, consequently, the heat flux estimate. Compared to $\hat{\varphi}_w$ obtained with the fast thermocouple results, the variations of the estimated values with the slow thermocouple were smaller in the first two seconds and the values decreased almost monotonously until 14 s, in a sequence of underestimated and overestimated $\hat{\varphi}_w$ during this time. In turn, the reconstructed signal, although being noisy, provided much better estimate of $\hat{\varphi}_w$, following well all the transients that were captured by the fast thermocouple. The calculated $\hat{\varphi}_w$ at the first peak demonstrates again the advantage of using the reconstructed signal in the inverse method: using the slow thermocouple data resulted in underestimating $\hat{\varphi}_w$ by 60.8%, while using the reconstructed signal deviated by only 1.7%. Table 3 presents these deviations of the calculated heat flux at the first peak from the estimated with the fast thermocouple data, as well as the normalized root-mean-square (RMS) error e_{RMS} using the fast thermocouple results as reference, which is calculated by:

$$e_{RMS} = \frac{1}{\hat{\varphi}_{w,max,fast}} \sqrt{\frac{\sum_{k=1}^{N_t} \left(\hat{\varphi}_{w,k} - \hat{\varphi}_{w,k,fast}\right)^2}{N_t}} \tag{15}$$

where $\hat{\varphi}_{w,max,fast}$, the maximal estimated heat flux using the fast thermocouple data, is the normalization parameter. Even though using the reconstructed signal improves globally the heat flux estimate, reducing by less than half e_{RMS} compared to the slow thermocouple results, the best benefit is found when estimating peak values where the calculation becomes much more accurate, demonstrating the benefits of correcting the thermocouple signal for estimating the heat flux at the boundary.

Table 3: Normalized RMS error of $\hat{\varphi}_w$ (Eq. 15) and deviation of the estimated heat flux at the first peak using the slow and reconstructed signals compared with the obtained with the fast thermocouple data.

Test	e_{RMS}		**First φ_w peak**	
	Slow	***Rec.***	***Slow***	***Rec.***
1	4.1%	1.8%	-21.4%	6.1%
2	4.8%	1.9%	-27.1%	7.5%
3	9.6%	4.3%	-61.7%	1.8%

3.3. Neglecting heat losses in the signal reconstruction

The thermocouple signal reconstruction with the present method starts by reproducing the instrumentation procedure of a main large-scale experimental campaign, where the slow thermocouple would be used, in a smaller scale where the fast and slow thermocouple measurements could be compared, as we performed in the previous section. In fact, the previous test was not arbitrary: the slow thermocouple and instrumentation method is similar to the ones we used in a previous study [14] that we discuss in more detail in section 3. Although the thermocouple characteristics and insertion geometry can be easily reproduced, which are responsible for the response time, the same is not true for the heat loss characteristics because, for instance, the sample temperature gradient that can vary with the test condition or heat flux at the boundary. Therefore, we could expect that the estimated response time $\hat{\tau}$ remains the same in the experimental campaign and in the small-scale test, but the estimated heat loss parameters $\hat{\xi}$ and $\hat{\theta}_{ref}$ may be different.

For this reason, we analyzed in Fig. 8 the sensitivity of the temperature signal reconstruction in Eq. 14 to the estimated parameters $\beta = \hat{\tau}$ and $\beta = \hat{\xi}$. The product $\beta\left(\partial\hat{\theta}_P/\partial\beta\right)$ gives the contribution of the parameter β to the calculation of $\hat{\theta}_P$. We chose two values for $\hat{\tau}$ (0.35 and 2.4 s, corresponding to tests 1 and 3, respectively) and one for $\hat{\xi}$ (0.05, an average of the three tests) to illustrate their sensitivities. The reference temperature was not analyzed because its sensitivity is constant in Eq. 14 ($\partial\hat{\theta}_P/\partial\hat{\theta}_{ref} = -\hat{\xi}$), but its effect is present in the sensitivity of $\hat{\xi}$ through the difference $\theta_{TC} - \hat{\theta}_{ref}$. The results show the thermocouple signal reconstruction is much more sensitive to $\hat{\tau}$ than to $\hat{\xi}$. In fact, the sensitivity to $\hat{\xi}$ is important solely when temperature derivative $d\hat{\theta}_{TC}/dt$ is very low. For example, the contribution of the heat loss when $\theta_{TC} - \hat{\theta}_{ref} = 20$ °C, which is close to the highest value we observed in our experiments ($\theta_{TC} \approx 40$ °C and $\hat{\theta}_{ref} \approx 20$ °C), is about the same as the response time contribution only when $d\hat{\theta}_{TC}/dt$ is lower than 3 °C/s and 0.5 °C/s for $\hat{\tau}$ equal to 0.35 s and 2.4 s, respectively. These values are much lower than the peak temperature derivatives measured in our experiments (about 60 °C/s), where the heat loss contributes to the signal reconstruction by less than 5% for $\hat{\tau} = 0.35$ s and 0.7% for $\hat{\tau} = 2.4$ s.

Therefore, if we are interested in estimating the heat flux rather than perfectly reconstructing the thermocouple signal, we could neglect the heat loss contribution in the signal reconstruction by setting $\hat{\xi} = 0$. Figure 9 presents how this assumption affects the signal reconstruction (a) and the heat flux estimation (b) for the validation tests 1 and 3 in the first ten seconds, where we have both intense and mild transient processes. For test 1, the original reconstructed signal is practically the same as the new reconstruction (i.e. with $\hat{\xi} = 0$) in the first two seconds where the temperature increase is steeper, both of them agreeing with the fast thermocouple measurement (Fig. 9a).

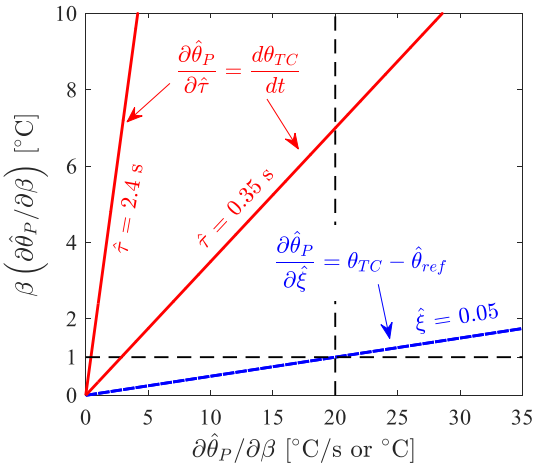

Figure 8: Sensitivity to $\hat{\tau}$ and $\hat{\xi}$ in the thermocouple signal reconstruction (Eq. 14) for $\hat{\tau} = 2.4$ s, $\hat{\tau} = 0.35$ s and $\hat{\xi} = 0.05$. The letter β represents the model parameter under analysis, thus either $\hat{\tau}$ or $\hat{\xi}$.

After 3 s, the temperature increase is much slower and the new reconstruction starts to deviate from the original one and tends to the slow thermocouple measurement. This complies with the analysis made with Fig.8: the heat loss contribution is negligible when the temperature derivative is high but it plays a role when it is lower. Nevertheless, this slight deviation between both reconstructions has virtually no effect on the heat flux estimation (Fig. 9b). The results with test 3 also confirm the sensitivity analysis since the heat loss contribution is practically nonexistent because the response time is very high. Consequently, both reconstructed signals superpose each other, as well as their corresponding estimated heat fluxes.

In conclusion, neglecting the heat loss contribution is an acceptable option to estimate the heat flux at the boundary, especially because, as already mentioned, this effect is more difficult to be reproduced in a small-scale experiment. On the other hand, the response time has a very important effect on the signal reconstruction and heat flux estimation, so it is important to reproduce as best as possible the geometry and instrumentation procedure of the main experimental campaign in the calibration test.

3.4. Noise and filtering effects analysis

Once having validated the method with experiments, we performed some simulations to evaluate how the noise level of thermocouple measurements and the application of data filtering would affect the response time estimation. Since its calculation depends on the difference between the fast and slow thermocouple measurements (Eq. 12) and the temperature derivative of the slow thermocouple (Eq. 11) – obtained using data regression of its temperature measurements (Eq. 8), one could expect that the response time estimation with Eq. 13 would be degraded if the noise measurements are high. Furthermore, data filtering could be used to reduce the measurement noise but would result in filtering as well high frequency processes, reducing the signal amplitude during fast transients of the calibration data. As we discussed before, this signal has a short duration in the calibration procedure adopted in this study (Fig. 5b and c), so one could also expect data filtering playing a role on the response time estimation.

The simulations were performed based on the calibration results of test 1, considering the 1D heat conduction model presented in Appendix A, and followed these steps:

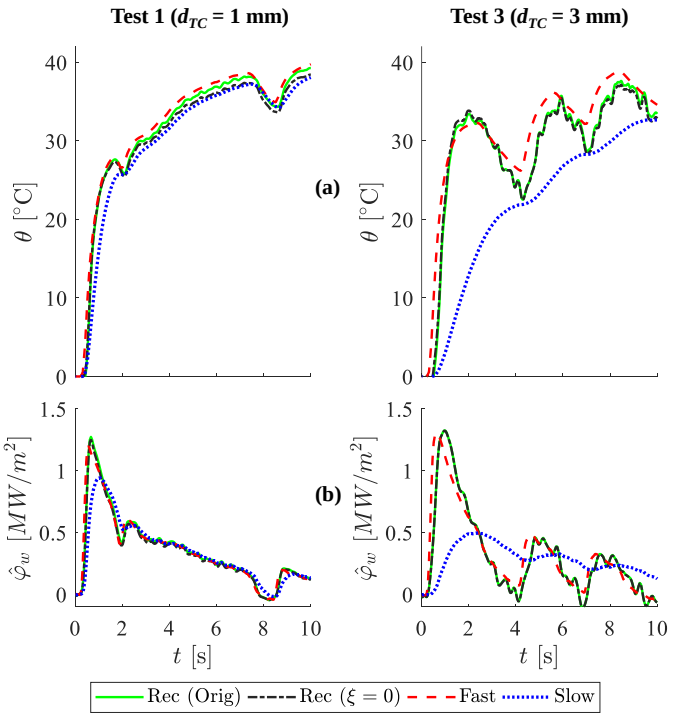

Figure 9: Analysis of the heat loss parameters effect on the signal reconstruction (a) and the heat flux estimation (b). Data for "Rec (Orig)" includes the estimated heat loss parameters, while for "Rec ($\xi = 0$)" the heat loss is neglected.

1. The estimated heat flux using the fast thermocouple (Fig. 7a) was applied at one surface while to other was considered insulated. In these conditions, the direct problem heat conduction problem was solved (Eq. A.2), calculating the temperature at the thermocouple position. This result is represented by a solid blue line in Fig. 10a, which corresponds to the condition with no response time ($\tau = 0$ s). Note it fits well the experimental result of the fast thermocouple response during the calibration step of test 1;
2. To simulate the thermocouple response time on the temperature measurements, the calculated temperature in the previous step was modified using Eq. 3, hence $\xi = 0$, resulting in temperature responses for different τ (other curves in Fig. 10a);
3. Next, a white noise ε was added to the temperature responses, whose value was randomly determined following a Gaussian distribution with zero mean value and a given standard deviation of σ_ε (examples of noises are shown in Fig. 10b). At this step, the simulated thermocouple measurement is completed, considering both the response time effect and the presence of measurement noise.
4. Before using these noisy simulated temperature responses for the response time estimation, we passed a convolutive Gaussian filter on the temperature data. We tested three different filtering conditions by varying the number of non-zero points n_G in the Gaussian profile (Fig. 10c): 1 (i.e. no filtering), 21 and 51. We should remind that $\sum w_k = 1$;
5. Finally, the thermocouple response time is estimated using the filtered noisy data and applying Eq. 13, where the data for $\tau = 0$ s acts as the fast thermocouple result (reference);
6. This procedure was repeated ten times for each calculation to evaluate the repeatability of the estimated response time. For each calculation, step 3 was repeated to have different noise values to add to the noiseless

temperature data. Therefore, each estimation had a particular simulated temperature signal, as we would have by repeating the same experiment several times.

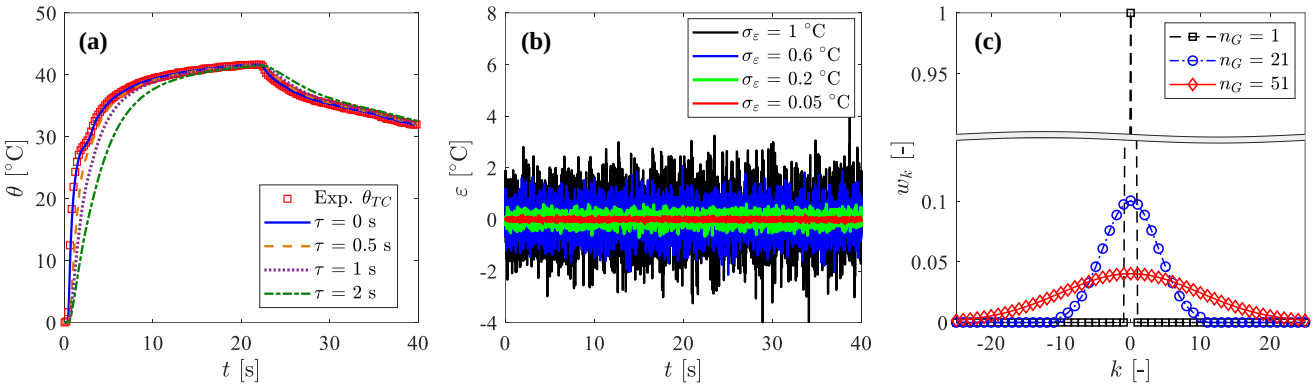

Figure 10: Simulation study of the noise and filtering effects based on test 1 calibration data: a) simulated temperature signals (lines) with different imposed response times (τ), as well as the experimental result of test 1 to show good match with the simulation with $\tau = 0$ s; b) example of temperature noise ε added to the temperature signal for different Gaussian standard deviations (σ_ε); c) weight profiles of the convolutive Gaussian filters used in this analysis, n_G being the number of non-zero points.

Figure 11 presents the estimated response times $\hat{\tau}$ for each imposed response time τ to the temperature measurement (step 2), imposed standard deviation σ_ε for the noise level (step 3) and number of non-zero data n_G for the Gaussian filter before calculating $\hat{\tau}$ (step 4). If the temperature measurements are noiseless, the estimated response time matches perfectly the imposed value, which was expected as the response time estimation is exactly the opposite equation of that generates the delayed temperature measurements. Once noise is present in the temperature measurements, $\hat{\tau}$ is no longer equal to τ and the estimated value varies for each repeated simulation. If $\tau = 0$, $\hat{\tau}$ is always calculated near zero with very little variance, regardless of the noise level or if data filtering is used. For $\tau > 0$, the increase in the noise level affects the accuracy of the response time estimation. More precisely, either using data filtering or not, the increase in the noise level tends to result in underestimated response times and to increase the uncertainty of $\hat{\tau}$. Finally, filtering the noisy temperature measurement is always beneficial for the response time estimation, in some cases even allowing accurate $\hat{\tau}$ calculations with filtered data that was much underestimated when using unfiltered data (see, for instance, the case with $\tau = 2$ s and $\sigma_\varepsilon = 0.2$ °C). In our experiments, we had $\sigma_\varepsilon = 0.2$ °C and we used data filtering with $n_G = 51$, ensuring accurate estimates in our test cases.

3.5. Application in a previous jet-cooling experiment

We finish this study applying our proposed method to reconstruct the thermocouple signal with experimental data from a previous study [14] of single-jet cooling near industrial conditions of a large hot nickel plate initially at about 850°C. We took results for the lowest and the highest jet Reynolds number that were tested (9,800 and 120,000, respectively) and temperature measurements at the impact location, where there is no transverse heat flux so the heat flux can be estimated solving an 1D inverse problem as in Appendix A. In that study, the sample was instrumented with type-N ungrounded sheathed thermocouples of 1 mm diameter. Therefore, we could estimate their response time to be similar to our test cases 1 and 2, so we assigned both a minimal and maximal response

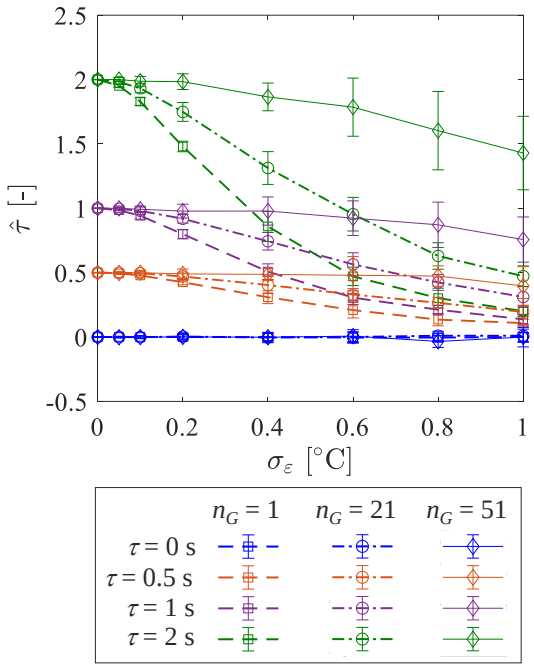

Figure 11: Estimated response times of the thermocouple for different imposed response times (τ), noise standard deviations (σ_ε) and Gaussian filtering profiles (n_G).

time value, $\tau_{min} = 0.35$ s and $\tau_{max} = 0.5$ s, respectively. We also neglected the heat loss contribution as studied in section 3.3, so we set $\xi = 0$.

Figure 12a presents the temperature decrease ($\theta = T - T_0$) in the first 10 s of the experiment, where the symbols correspond to the original experimental temperature measurements and the lines to the reconstructed signal using τ_{min} (dotted lines) and τ_{max} (dashed lines). The zone between both lines was shaded to better visualize the range we would obtain with intermediary values of response time. The temperatures of the reconstructed signals decrease substantially faster than the original signals just after the beginning of the jet impingement cooling, an expected behavior as we saw in the previous sections. The difference between the original and reconstructed temperatures reached 160°C about 0.5 s after starting the cooling, which confirms an analysis in the previous paper [14] of measuring rewetting temperatures much higher than the thermodynamic limit of liquid superheat because of the thermocouple response time (among other factors). At about 10 s, the original and reconstructed signals match again, which can be a consequence of having neglected the heat loss contribution.

In turn, Fig. 12b presents the estimated heat flux at the surface using both the original (filled lines) and reconstructed (dotted and dashed lines, as before) temperature measurements. The increase in the estimated heat flux using the reconstructed signals is smaller for the lowest Re_j (7.9% and 26.3% using data with τ_{min} and τ_{max}, respectively) than for the highest (24.5% and 59.2% respectively for τ_{min} and τ_{max}). This is because, for the latter case, the heat fluxes are higher and, consequently, the temperature transients are faster. Therefore, these higher temperature derivatives become even higher with the response time correction (Eq. 14), resulting is a substantial increase in the estimated heat flux with the inverse method.

Finally, we highlight another consequence of the thermocouple response time in transient heat transfer studies. Not only does it damper the temperature response that results in underestimated heat fluxes at the boundary, but

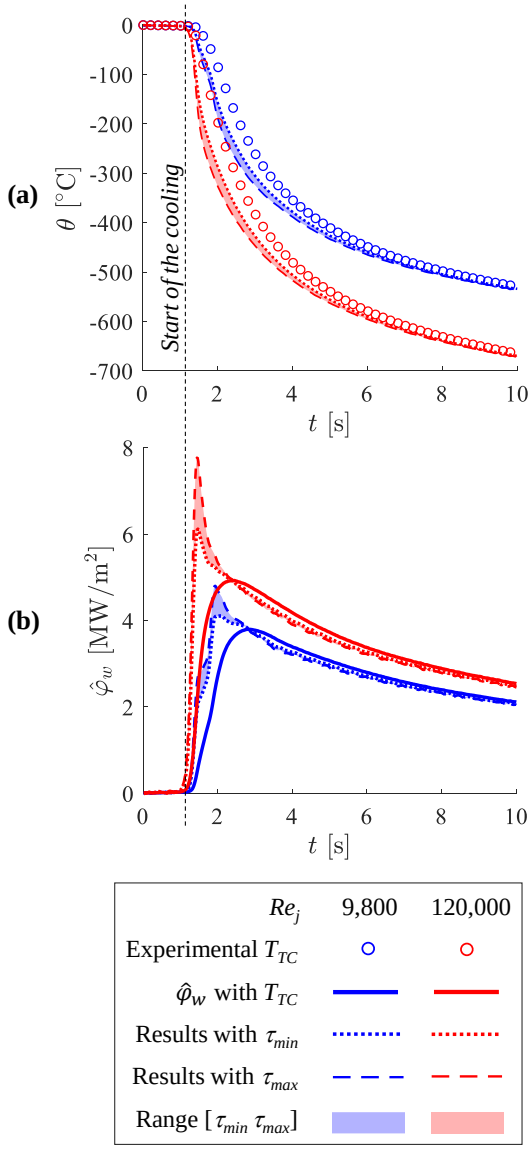

Figure 12: Application of the present thermocouple signal reconstruction in a previous hot-metal jet impingement cooling test [14] using $\tau_{min} = 0.35$ s and $\tau_{max} = 0.5$ s: a) temperature evolution; b) estimated heat flux at the boundary.

also the response time can hide the importance of parametric effects under study. When analyzing the effect of the Reynolds number in Fig. 12b using $\hat{\varphi}_w$ obtained with the original data, we would have affirmed that the rise in Re_j from 9,800 to 120,000 increased the peak of the dissipated heat flux at impact by only 29%. Nevertheless, using results of the reconstructed signals, this increase rises to between 49% (using data for τ_{min}) and 63% (data for τ_{max}), showing Re_j plays a more important role than initially observed. This is particularly critical because a parameter can be judged less or even not important while it can actually affect substantially the cooling process.

4. Conclusions

In this study, we analyzed the difference between temperature measurements by thermocouples with different response times, especially in fast transients. In order to correct the temperature response of slow thermocouples, and to avoid underestimation of the estimated heat fluxes with inverse methods, several steps were performed:

1. The temperature evolution of a thermocouple was modeled, including its response time and heat loss at the hot junction. After a parametric sensitivity study, it was found that the heat losses can actually be neglected in fast transients where the temperature derivative is high; however, they play a non-negligible role when the derivative is low. Nevertheless, if the main objective is estimating the heat flux from temperature measurements, the heat loss can be completely neglected;
2. A least squares method was presented to estimate the model parameters (more precisely, the thermocouple response time, the thermal resistance ratio and the reference temperature) using experimental measurements of two thermocouples with different response times: one named "slow" with high response time; and one named "fast" with low response time. In this study, we tested the proposed method with a heated jet impingement experiment, where the parameters were estimated in a calibration test and validated afterwards using the estimated parameters to reconstruct the slow thermocouple signal, which matched well the fast thermocouple measurements;
3. An analysis of the temperature measurement noise effect demonstrated that high noises lead to underestimated response times; however, this problem can be partially or completely mitigated by filtering the thermocouple data;
4. Finally, the proposed method was applied to a large-scale jet cooling experiment of a hot nickel plate, whose results were published in a previous study. The heat fluxes estimated using the reconstructed thermocouple signals were substantially higher than the ones initially estimated using the original measurements, which highlighted a more important effect of the jet Reynolds number than what was observed before.

As the present method demonstrated to be effective, we encourage using corrected temperature measurements in future studies involving fast thermal transients to have more accurate estimates of the boundary heat flux. This would provide data less dependent of the instrumentation method and would possibly allow comparing with results from other experiments in the literature.

5. Funding

This study was performed using funding of Laboratoire Énergies & Mécanique Théorique et Appliquée (LEMTA), in the University of Lorraine, France.

References

[1] R. Lemaire, S. Menanteau, Assessment of radiation correction methods for bare bead thermocouples in a combustion environment, International Journal of Thermal Sciences 122 (2017) 186–200. doi:https://doi.org/10.1016/j.ijthermalsci.2017.08.014.

[2] I. Pope, J. P. Hidalgo, J. L. Torero, A correction method for thermal disturbances induced by thermocouples in a low-conductivity charring material, Fire Safety Journal 120 (2021) 103077, fire Safety Science: Proceedings of the 13th International Symposium. doi:https://doi.org/10.1016/j.firesaf.2020.103077.

[3] A. Terzis, J. von Wolfersdorf, B. Weigand, P. Ott, Thermocouple thermal inertia effects on impingement heat transfer experiments using the transient liquid crystal technique, Measurement Science and Technology 23 (11) (2012) 115303. doi:https://doi.org/10.1088/0957-0233/23/11/115303.

[4] H. Hashemian, K. Petersen, D. Mitchell, M. Hashemian, D. Beverly, In situ response time testing of thermocouples, ISA Transactions 29 (4) (1990) 97–104. doi:https://doi.org/10.1016/0019-0578(90)90046-N.

[5] K. Zhou, J. Qian, N. Liu, S. Zhang, Validity evaluation on temperature correction methods by thermocouples with different bead diameters and application of corrected temperature, International Journal of Thermal Sciences 125 (2018) 305–312. doi:https://doi.org/10.1016/j.ijthermalsci.2017.12.002.

[6] G. E. Daniels, Measurement of gas temperature and the radiation compensating thermocouple, Journal of Applied Meteorology and Climatology 7 (6) (1968) 1026 – 1035. doi:https://doi.org/10.1175/1520-0450(1968)007<1026:MOGTAT>2.0.CO;2.

[7] S. Brohez, C. Delvosalle, G. Marlair, A two-thermocouples probe for radiation corrections of measured temperatures in compartment fires, Fire Safety Journal 39 (5) (2004) 399–411. doi:https://doi.org/10.1016/j.firesaf.2004.03.002.

[8] M. H. Attia, A. Cameron, L. Kops, Distortion in Thermal Field Around Inserted Thermocouples in Experimental Interfacial Studies, Part 4: End Effect , Journal of Manufacturing Science and Engineering 124 (1) (2000) 135–145. doi:https://doi.org/10.1115/1.1419199.

[9] R. J. Moffat, Describing the uncertainties in experimental results, Experimental Thermal and Fluid Science 1 (1) (1988) 3–17. doi:https://doi.org/10.1016/0894-1777(88)90043-X.

[10] P. L. Woodfield, M. Monde, Estimation of uncertainty in an analytical inverse heat conduction solution, Experimental Heat Transfer 22 (3) (2009) 129–143. doi:https://doi.org/10.1080/08916150902805968.

[11] A. Kossolapov, F. Chavagnat, R. Nop, N. Dorville, B. Phillips, J. Buongiorno, M. Bucci, The boiling crisis of water under exponentially escalating heat inputs in subcooled flow boiling at atmospheric pressure, International Journal of Heat and Mass Transfer 160 (2020) 120137. doi:https://doi.org/10.1016/j.ijheatmasstransfer.2020.120137.

[12] V. Scheiff, N. Baudin, P. Ruyer, J. Sebilleau, C. Colin, Transient flow boiling in a semi-annular duct: From the onset of nucleate boiling to the fully developed nucleate boiling, International Journal of Heat and Mass Transfer 138 (2019) 699–712. doi:https://doi.org/10.1016/j.ijheatmasstransfer.2019.04.069.

[13] A. Labergue, J.-D. Pena-Carillo, M. Gradeck, F. Lemoine, Combined three-color lif-pda measurements and infrared thermography applied to the study of the spray impingement on a heated surface above the leidenfrost regime, International Journal of Heat and Mass Transfer 104 (2017) 1008–1021. doi:https://doi.org/10.1016/j.ijheatmasstransfer.2016.07.029.

[14] A. V. S. Oliveira, D. Maréchal, J.-L. Borean, V. Schick, J. Teixeira, S. Denis, M. Gradeck, Experimental study of the heat transfer of single-jet impingement cooling onto a large heated plate near industrial conditions,

International Journal of Heat and Mass Transfer 104 (2021) 121998, accepted in 21/09/2021. doi:https://doi.org/10.1016/j.ijheatmasstransfer.2021.121998.

[15] A. H. Nobari, V. Prodanovic, M. Militzer, Heat transfer of a stationary steel plate during water jet impingement cooling, International Journal of Heat and Mass Transfer 101 (2016) 1138 – 1150. doi:https://doi.org/10.1016/j.ijheatmasstransfer.2016.05.108.
URL http://www.sciencedirect.com/science/article/pii/S0017931015313594

[16] M. Gradeck, J. Ouattara, B. Rémy, D. Maillet, Solution of an inverse problem in the hankel space – infrared thermography applied to estimation of a transient cooling flux, Experimental Thermal and Fluid Science 36 (2012) 56–64. doi:https://doi.org/10.1016/j.expthermflusci.2011.08.003.

[17] N. Karwa, P. Stephan, Experimental investigation of free-surface jet impingement quenching process, International Journal of Heat and Mass Transfer 64 (2013) 1118 – 1126. doi:https://doi.org/10.1016/j.ijheatmasstransfer.2013.05.014.

[18] B. Wang, D. Lin, Q. Xie, Z. Wang, G. Wang, Heat transfer characteristics during jet impingement on a high-temperature plate surface, Applied Thermal Engineering 100 (2016) 902 – 910. doi:https://doi.org/10.1016/j.applthermaleng.2016.02.054.

[19] Y. Xian, P. Zhang, S. Zhai, P. Yang, Z. Zheng, Re-estimation of thermal contact resistance considering near-field thermal radiation effect, Applied Thermal Engineering 157 (2019) 113601. doi:https://doi.org/10.1016/j.applthermaleng.2019.04.011.

[20] S. Kumar, A. Tariq, Determination of thermal contact conductance of flat and curvilinear contacts by transient approach, Experimental Thermal and Fluid Science 88 (2017) 261–276. doi:https://doi.org/10.1016/j.expthermflusci.2017.06.004.

[21] F. Van Breugel, J. N. Kutz, B. W. Brunton, Numerical differentiation of noisy data: A unifying multi-objective optimization framework, IEEE Access 8 (2020) 196865–196877. doi:https://doi.org/10.1109/ACCESS.2020.3034077.

[22] I. Knowles, R. J. Renka, Methods for numerical differentiation of noisy data, in: Variational and Topological Methods: Theory, Applications, Numerical Simulations, and Open Problems. Electron. J. Diff. Eqns., Conference 21, 2014, pp. 235–246.

[23] A. Savitzky, M. J. E. Golay, Smoothing and differentiation of data by simplified least squares procedures., Analytical Chemistry 36 (8) (1964) 1627–1639. doi:https://doi.org/10.1021/ac60214a047.

[24] A. Lecoanet, F. Payot, C. Journeau, N. Rimbert, M. Gradeck, Study of the ablation consecutive to jet impingement on a meltable solid – application to SFR core-catcher, Nuclear Engineering and Design 377 (2021) 111147. doi:https://doi.org/10.1016/j.nucengdes.2021.111147.

[25] D. J. Womac, S. Ramadhyani, F. P. Incropera, Correlating Equations for Impingement Cooling of Small Heat Sources With Single Circular Liquid Jets, Journal of Heat Transfer 115 (1) (1993) 106–115. doi:https://doi.org/10.1115/1.2910635.

[26] M. N. Õzişik, Heat Conduction, Wiley-Interscience publication, John Wiley & Sons, 1993.

[27] D. Maillet, S. André, J. C. Batsale, A. Degiovanni, C. Moyne, Thermal Quadrupoles: Solving the Heat Equation through Integral Transforms, John Wiley & Sons, 2000.

[28] A. V. S. Oliveira, C. Zacharie, B. Rémy, V. Schick, D. Maréchal, J. Teixeira, S. Denis, M. Gradeck, Inverse ARX (IARX) method for boundary specification in heat conduction problems, International Journal of Heat and Mass Transfer 180 (2021) 121783. doi:https://doi.org/10.1016/j.ijheatmasstransfer.2021.121783.

[29] H. Stehfest, Algorithm 368: Numerical inversion of laplace transforms [d5], Commun. ACM 13 (1) (1970) 47–49. doi:10.1145/361953.361969.

[30] J. V. Beck, B. Blackwell, C. R. St. Clair Jr., Inverse Heat Conduction: Ill-Posed Problems, Wiley-Interscience publication, John Wiley & Sons, 1985.

Appendix A. 1D heat conduction modeling and inverse method

Figure A.13 presents the 1D heat conduction problem used to model our experiment, which consists of a body with a transient heat flux $\varphi_w(t)$ as boundary condition at $x = 0$ and insulated surface at $x = L$, where L is the length of the body (in our tests, $L = 28$ mm). A virtual thermocouple TC is located at x_{TC}, which is 1 mm in our test cases.

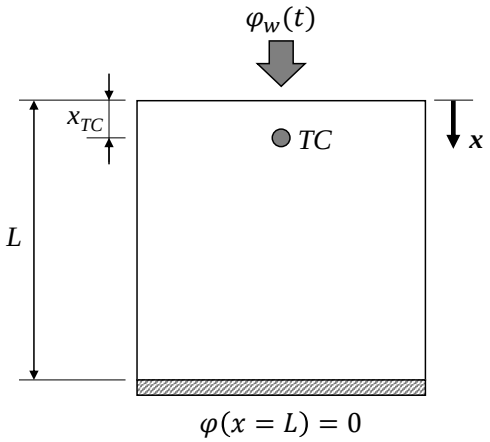

Figure A.13: Schematic drawing of the 1D heat conduction problem.

The temperature evolution is found by solving the following heat equation, considering constant thermophysical properties:

$$\frac{\partial^2 \theta}{\partial x^2} = \frac{1}{a}\frac{\partial \theta}{\partial t} \tag{A.1}$$

$\theta = T - T_0$ being the temperature difference from the body initial temperature T_0 and $a = \lambda\rho^{-1}c_p^{-1}$ is the thermal diffusivity (λ, ρ and c_p are, respectively, the material's thermal conductivity, density and specific heat). Among several methods that can be used to solve this equation [26], we chose the thermal quadrupoles method [27] applying the Duhamel's theorem [26] that considers the heat flux $\varphi_w(t)$ constant by parts, i.e. at each time step, as performed in a previous study [28]. This results in the following expression for the temperature at the thermocouple position:

$$\theta_{TC}(t_{k+1}) = \sum_{j=0}^{k} X(x_{TC}, t_{k-j})\varphi(t_j) \tag{A.2}$$

where:

$$X(x_{TC}, t_k) = -\frac{1}{\lambda}\int_{t_k}^{t_{k+1}} Z(x_{TC}, \tau)d\tau \tag{A.3}$$

Z being a function in the time domain obtained using the Stehfest algorithm [29] for the Laplace transform inversion of the following expression:

$$Z = \mathcal{L}^{-1}\left\{\frac{1}{\sqrt{\frac{p}{a}}}\left[\frac{\cosh\left(\sqrt{\frac{p}{a}}L\right)}{\sinh\left(\sqrt{\frac{p}{a}}L\right)}\cosh\left(\sqrt{\frac{p}{a}}x_{TC}\right) - \sinh\left(\sqrt{\frac{p}{a}}x_{TC}\right)\right]\right\} \tag{A.4}$$

where p is the Laplace variable.

Equation A.2, the solution of the direct problem, is the one used to generate the simulated temperature responses in the introduction (Fig. 1) and for the analysis in section 3.4 from a known imposed heat flux $\varphi_w(t)$ (Fig. 10a). The estimation of the heat flux from temperature measurements is an inverse problem that could theoretically be solved by simply isolating $\varphi_w(i, t_k)$ in Eq. A.2, that is:

$$X(t_0)\hat{\varphi}(t_k) = \theta_{TC}(t_{k+1}) - \sum_{j=0}^{k-1} X(t_{k-j+1})\hat{\varphi}(t_j) \tag{A.5}$$

where we consider that all the previous heat fluxes $\hat{\varphi}(t_j)$ has already been estimated. However, because of the ill-posed nature of the problem, small variations in the temperature measurements due to embedded noises make this calculation diverge. A regularization method becomes necessary, so we used Beck's function specification method [30], which filters the temperature signal by assigning a functional for the n_{fts} future heat fluxes to estimate the present heat flux. In this study, we used the simplest functional, which is considering the heat fluxes at the time steps $k + n_{fts}$ equal to the heat flux being estimated at the time step k, i.e. $\hat{\varphi}(t_k) = \hat{\varphi}(t_{k+1}) = ... = \hat{\varphi}(t_{k+n_{fts}})$. For this purpose, we must have available temperature measurements of the next $k + 1 + n_{fts}$ time steps. Equation A.5 can thus be written for each future time step as follows:

$$\left(\sum_{j=1}^{n_{fts}} X_j\right)\hat{\varphi}(t_k) = \theta(t_{k+n_{fts}}) - \sum_{j=0}^{k-1} X(x_{TC}, t_{k-j+n_{fts}})\hat{\varphi}(t_j) \tag{A.6}$$

This creates a system of n_{fts} equations that can be presented in the following matrix form:

$$\mathbf{S}_{fts}\hat{\varphi}(t_k) = \mathbf{D}_{fts} \tag{A.7}$$

$\mathbf{S}_{fts}$ is the sensitivity vector whose elements are the left term of Eq. A.6 for each future time step, while $\mathbf{D}_{fts}$ is the result vector also calculated composed of the terms in the right of Eq. A.6 for each future time step. The calculation of $\hat{\phi}[k]$ is finally done by the least squares method:

$$\hat{\varphi}(t_k) = \left(\mathbf{S}_{fts}^T \mathbf{X} \mathbf{S}_{fts}\right)^{-1} \mathbf{S}_{fts}^T \mathbf{D}_{fts} \tag{A.8}$$

This calculation is repeated for the next time steps until the last time step, which is $N_t - n_{fts}$ since no future temperature measurements is available to estimate heat fluxes after this point. The estimated heat fluxes presented in Figs. 7, 9b and 12b were obtained with Eq. A.8.

Appendix B. MatLab code of the proposed method in the supplementary material

In the supplementary material, we provide the MatLab code "CorrectionTC.m" we developed to estimate the thermocouple response time τ and the heat loss parameters ξ and T_{ref} with experimental data (calibration), as well as the thermocouple reconstruction signal once these parameters are given (validation). Note that, in the code, the signal reconstruction can be performed using different values of τ, ξ and θ_{ref} than the ones estimated during calibration. The code is entirely commented for better usability and understanding of the parameters. The input parameters necessary for running the code are all listed in the beginning and the code runs using data provided in a text file. The code can be easily modified to accept other file extensions, like an Excel sheet. We also provided four experimental data examples: two sets of calibration ("Test1Calib.txt" and "Test3Calib.txt") and validation data ("Test1Valid.txt" and "Test3Valid.txt") that were used to plot the curves in Figs. 5 and 6.

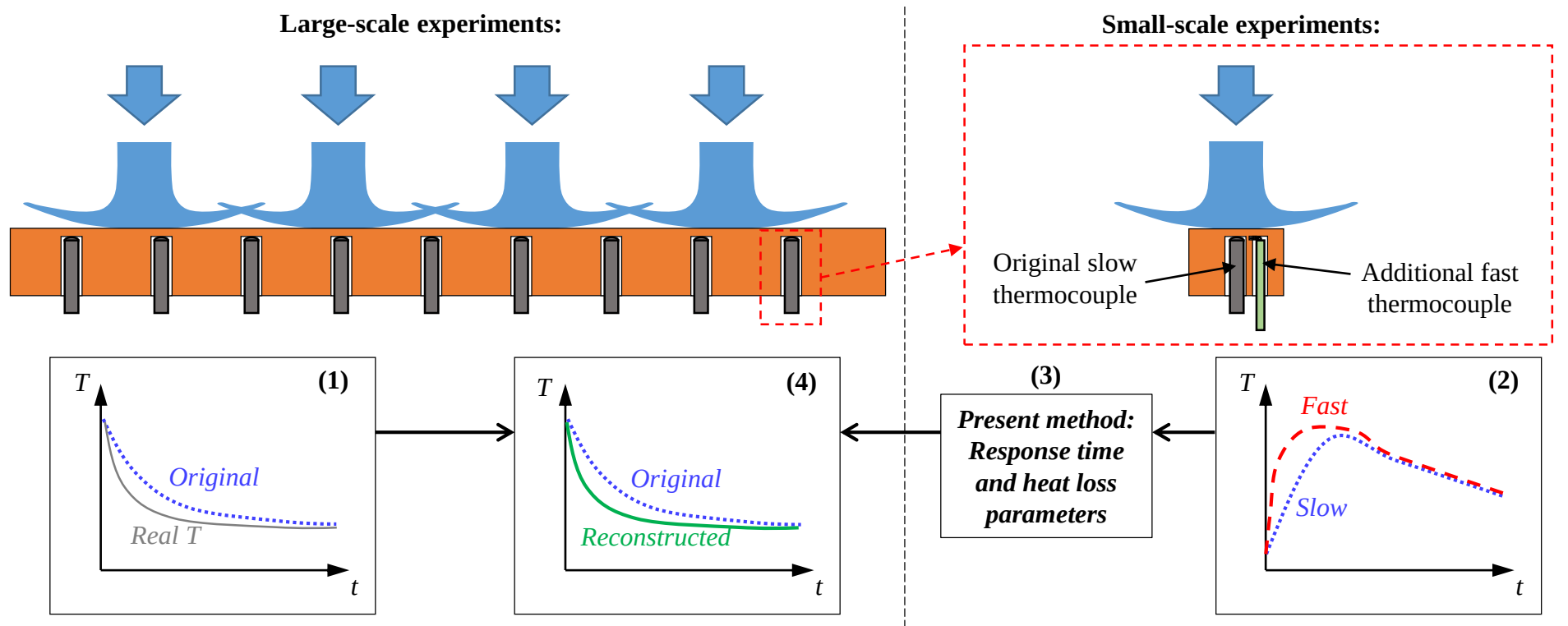
Large-scale experiments:
Small-scale experiments:
Original slow thermocouple
Additional fast thermocouple
T
(1)
Original
Real T
t
T
(4)
Original
Reconstructed
t
(3)
Present method: Response time and heat loss parameters
T
(2)
Fast
Slow
t